Iran J Sci Technol Trans Civ Eng (2018) 42:17–32
https://doi.org/10.1007/s40996-017-0083-y

RESEARCH PAPER

A Family of Cubic B-Spline Direct Integration Algorithms with Controllable Numerical Dissipation and Dispersion for Structural Dynamics

S. Rostami[1] · S. Shojaee[1]

Received: 24 November 2016 / Accepted: 2 November 2017 / Published online: 11 November 2017

Abstract In recent years, a conditionally stable explicit time integration scheme using cubic B-spline function has been proposed for solving the problems in structural dynamics. The current paper presents a scheme where this method is developed to an efficient implicit unconditionally stable time integration method. In this research, in order to apply the stabilization process, first, a series of implicit standard formulas were derived from previous explicit formulation. Then after inserting two controlling parameters γ and β in the standard formulas, unconditional stability is guaranteed. The values of these two parameters have been determined to not only maintain the stability but also ensure the desired accuracy. Finally, for the new method, a simple step-by-step algorithm is presented. Stability and accuracy analysis of the proposed algorithm has been completely investigated. The efficiency and computational cost of the proposed method are demonstrated through two numerical simulations. Compared with those from some of the existing numerical methods in the literature, such as the Bathe method, the proposed method has higher computation efficiency with less time consumption.

Keywords Cubic B-spline · Time integration · Implicit · Unconditional stability · Consistency · Dissipation · Dispersion

✉ S. Shojaee
Saeed.shojaee@uk.ac.ir

[1] Department of Civil Engineering, Shahid Bahonar University of Kerman, Kerman, Iran

1 Introduction

Step-by-step direct time integration algorithms are widely used in the computational analysis of structural dynamics and transient wave propagation problems. Efficient and accurate numerical integration methods have been and continue to be the focus of considerable attention because they have an inherent simplicity in solving problems of structural dynamics and are the only tools to obtain solutions to general nonlinear structural dynamics problems. For reliable solution, a stable and efficient integration algorithm is desirable.

Generally, there are two basic categories of step-by-step integration methods. A time integration method is implicit if the solution procedure requires the factorization of an 'effective stiffness' matrix and is explicit otherwise (Dokainish and Subbaraj 1989; Subbaraj and Dokainish 1989). Both explicit and implicit methods have their own advantages and disadvantages. Implicit methods require a much larger computational effort per time step when compared with explicit methods.

Stability is the most important characteristic of a time integration method. Depending on the stability characteristic, integration algorithms are classified as either unconditionally or conditionally stable, where unconditional stability implies that the numerical solution of a free-vibration problem with any arbitrary initial conditions does not grow without bound for any integration time step size (Bathe 1996). The implicit methods can be designed to have unconditional stability, in linear analysis, so that the time step size can be selected only based on the characteristics of the problem to be solved. On the other hand, explicit methods when using a diagonal mass matrix may require only vector calculations. Hence, the computational cost per time step is much lower. However, an explicit method can only be conditionally stable. Therefore, explicit methods may be effective when the time step size required by the stability limit is about the same as the time step size needed to describe the physical problem, and this is frequently the case in wave propagation analyses. More details of time integration methods can be found in Bathe (1996) and Chopra (2007) and the references therein.

Various different time integration algorithms have been proposed. The oldest and most powerful algorithms include the Newmark family of integration algorithms (Newmark 1959), Wilson method (Wilson et al. 1973; Wilson 1986) and Hilber-Hughes-Taylor α-method (Hilber et al. 1977). Today also new efficient methods are being developed. For example, Kolay and Ricles (2014) developed a family of unconditionally stable direct integration algorithms with controllable numerical energy dissipation as the explicit KR-α method and Soleymani et al. (2009) proposed a time integration algorithm for linear transient analysis based on the reproducing kernel method. Recently, Bathe (2007) proposed an efficient time integration method for solving the problems in structural dynamics and wave propagation. Desirable performance of the Bathe method was demonstrated in a series of research papers (Bathe 2007; Bathe and Noh 2012; Noh and Bathe 2013). Bathe (2007) developed a simple implicit time integration method which can remain unconditionally stable without the use of adjustable parameters. This implicit method shows very desirable calculation accuracy and high-frequency dissipation characteristics. However, this method consists of two sub-steps within each time step and thus consumes much more computation time than other conventional methods. Subsequently, Noh and Bathe (2013) presented an explicit time integration method which possesses second-order accuracy for systems with and without damping. By use of two sub-steps within each time step, this scheme can achieve a desired numerical damping to suppress undesirable spurious oscillations of high frequencies.

The analysis of integration algorithms is typically carried out in the time domain. In accuracy evaluation of the time integration methods, usually two quantities are determined: dispersion and dissipation (Hilber and Hughes 1978). Dissipation (amplitude decay) and dispersion (period elongation) are two criteria used to evaluate the performance of an integration algorithm. Apart from numerical dissipation, it is desirable for the algorithms to possess unconditional stability so that time increment of any size can be adopted without introducing numerical instability. The stability and accuracy of different integration algorithms have been extensively studied using the amplification matrix and its associated eigenvalues (Belytschko and Hughes 1983). An efficient method is one which, despite the ability of high-frequency dissipation, neither causes loss of accuracy, nor introduces excessive algorithmic damping in important low frequency modes. Indeed, efficient algorithm creates some damping in a time integration method by use of adjustable parameters. Most of present-day time integration methods, such as the higher-order mixed method (Wang and Au 2004), the two-step lambda method (Leontyev 2010) and the Newmark-type integration schemes (Newmark 1959; Wood et al. 1981), have parameters that can control the degree of numerical dissipation as well as the stability and accuracy.

Application of cubic and quartic B-spline functions for the numerical solution of dynamic systems has been presented by Rostami and Shojaee in a series of papers (Shojaee et al. 2011, 2015; Rostami et al. 2012, 2013). Implementation of cubic B-spline for the numerical solution of SDOF dynamic systems was introduced by Shojaee et al. (2011). Then in another work (Rostami et al. 2013), the proposed method was generalized for MDOF systems. The proposed method operates well, but its shortcoming was its conditional stability. This paper introduces a new version of previous work (Rostami et al. 2013) and resolves the above mentioned shortcoming by creating controllable damping in the algorithm. In this study, the proposed method is regenerated and developed to an unconditionally stable state. The proposed method has appropriate convergence, accuracy and low time consumption. Accuracy and stability analysis has been done profoundly in that paper. This time integration method benefits from a high order accuracy compared to the methods in the literature.

As it is well known, the cost of an analysis is directly related to the size of the time step which has to be used for stability and accuracy. In this paper, an unconditionally stable scheme is presented which allows a relatively large time step to be used. Wen et al. (2014, 2015) proposed an explicit method by utilizing a family of uniform septuple and quintic B-splines. Wen's method possesses high calculation accuracy, but has complicated algorithm and consumes more computation time compared to other conventional methods due to its complex formulations, especially for the dynamic system with very large DOFs.

This paper is formed as follows. In the next section, we have a brief review of the cubic B-spline time integration method. Section 3 is devoted to derivation of new and standard form of formulas from previous formulation. Section 4 is allocated to developed method using stabilization process. Section 5 is assigned to properties analysis of the proposed implicit time integration method such as stability, convergence, dissipation and dispersion, and finally a step-by-step algorithm of the proposed method has been introduced at the end of this section. Finally in Sect. 6 the efficiency of the proposed method is demonstrated with two examples.

2 Cubic B-Spline Direct Time Integration Method

A conditionally stable explicit time integration scheme using cubic B-spline function was proposed by Shojaee et al. (2011) and Rostami et al. (2013), for solving the problems in structural dynamics. In the first paper (Shojaee et al. 2011), by use of periodic cubic B-spline interpolation polynomial, the authors proceeded to solve the differential equation of motion governing single-degree-of-freedom (SDOF) systems and later in the second paper (Rostami et al. 2013) proposed method was generalized for multi-degree-of-freedom (MDOF) systems. Finally after doing a series of algebraic operations, a straightforward formulation was derived from the approximation of the response of the system with B-spline basis. In order to access more content about this method, see (Rostami et al. 2013).

In the following, the complete step-by-step algorithm of this proposed method for dynamic analysis of SDOF systems is given in Table 1.

3 New Formulation

Before entering the stabilization stage of the proposed method, it is necessary to change the previous explicit form of formula into the new implicit formulation. To achieve this goal, it is required to perform a series of algebraic operations on previous formulas. At first, we solve the following equations in order to obtain C_{i-3} to C_{i-1}. These equations are derived from Table 1.

$$u(t_i) = \frac{1}{6}(C_{i-3} + 4C_{i-2} + C_{i-1}) \tag{1a}$$

$$\dot{u}(t_i) = \frac{1}{2\Delta t}(C_{i-1} - C_{i-3}) \tag{1b}$$

$$\ddot{u}(t_i) = \frac{1}{\Delta t^2}(C_{i-3} - 2C_{i-2} + C_{i-1}) \tag{1c}$$

So, having Eq. (1) in hand, it is possible to solve the system equations and write these three unknowns in terms of displacement, velocity, acceleration as

$$C_{i-1} = u_i + \Delta t\dot{u}_i + \frac{\Delta t^2}{3}\ddot{u}_i \tag{2a}$$

$$C_{i-2} = u_i - \frac{\Delta t^2}{6}\ddot{u}_i \tag{2b}$$

$$C_{i-3} = u_i - \Delta t\dot{u}_i + \frac{\Delta t^2}{3}\ddot{u}_i \tag{2c}$$

Setting Eq. (2a) at the current time (t) equal to Eq. (2b) at the next time $(t + \Delta t)$, we will get to

$$C_{i-1} = u_i + \Delta t\dot{u}_i + \frac{\Delta t^2}{3}\ddot{u}_i = u_{i+1} - \frac{\Delta t^2}{6}\ddot{u}_{i+1} \tag{3}$$

Table 1 Step-by-step solution using cubic B-spline direct integration method (for SDOF systems)

A. Initial calculation
Determine stiffness k, mass m and damping ratio ξ of the system
Specify the force value applied to the system in each time instant
Determine initial value of displacement u_0 and velocity v_0
Select appropriate time step ($\Delta t < \Delta t_{\text{critical}}$) and calculate constant parameters α, β and γ as
$\alpha = \left(\frac{1}{\Delta t^2} - \frac{\xi\omega}{\Delta t} + \frac{\omega^2}{6}\right)$
$\beta = \left(\frac{-2}{\Delta t^2} + \frac{2\omega^2}{3}\right)$
$\gamma = \left(\frac{1}{\Delta t^2} + \frac{\xi\omega}{\Delta t} + \frac{\omega^2}{6}\right)$ where $\omega = \sqrt{\frac{k}{m}}$
Using the terms below determine the values of three unknown coefficients (C_{-3}, C_{-2} and C_{-1});
$C_{-3} = \frac{\Delta t^2}{6}\left(-3\beta u_0 - \Delta t(4\gamma - \beta)v_0 + \frac{2F(t_0)}{m}\right)$
$C_{-2} = \frac{\Delta t^2}{6}\left(3(\gamma + \alpha)u_0 + \Delta t(\gamma - \alpha)v_0 - \frac{F(t_0)}{m}\right)$
$C_{-1} = \frac{\Delta t^2}{6}\left(-3\beta u_0 + \Delta t(\beta - 4\alpha)v_0 + \frac{2F(t_0)}{m}\right)$
B. For each time step ($i = 0,1,\ldots,n$)
Calculate displacement, velocity and acceleration simultaneously, by
$u(t_i) = \frac{1}{6}(C_{i-3} + 4C_{i-2} + C_{i-1})$
$\dot{u}(t_i) = \frac{1}{2\Delta t}(C_{i-1} - C_{i-3})$
$\ddot{u}(t_i) = \frac{1}{\Delta t^2}(C_{i-3} - 2C_{i-2} + C_{i-1})$
Calculate unknown coefficient C_i from $i = 0$ to $(n - 1)$ by
$C_i = \frac{1}{\gamma}\left(\frac{F(t_{i+1})}{m} - \alpha C_{i-2} - \beta C_{i-1}\right)$

Then if we arrange the above equation in terms of u_{i+1}, it can be expressed as

$$u_{i+1} = u_i + \Delta t\dot{u}_i + \frac{\Delta t^2}{6}(\ddot{u}_{i+1} + 2\ddot{u}_i) \tag{4}$$

Similarly, if we do this process for Eq. (2b) at the current time (t) and Eq. (2c) at the next time ($t + \Delta t$) and then arrange the outcome in terms of $\dot{u}_{i+1}$, we get to

$$\dot{u}_{i+1} = \dot{u}_i + \frac{\Delta t}{2}(\ddot{u}_{i+1} + \ddot{u}_i) \tag{5}$$

Now, having Eqs. (4) and (5) we can rewrite this equation in terms of $\Delta\ddot{u}_i$ as follows:

$$\Delta u_i = \Delta t\dot{u}_i + \frac{\Delta t^2}{2}\ddot{u} + \frac{\Delta t^2}{6}\Delta\ddot{u}_i \tag{6}$$

$$\Delta\dot{u}_i = \Delta t\ddot{u}_i + \frac{\Delta t}{2}\Delta\ddot{u}_i \tag{7}$$

The formulas obtained in the end of the above algebraic calculation have the same format as those standard equations of the methods in the literature. These new derived formulas are shorter than the similar formulas in the previous papers but have exactly the same performance as before. Having the new implicit equations, i.e., Eqs. (6) and (7), it is possible to implement stabilization process in order to provide unconditional stability.

4 The Proposed Method; Modified Cubic B-Spline

Existence of one or two independent parameters in time integration methods can control the behavior of numerical method, so by adjusting the values of these parameters, stability of integration method is satisfied even in a large time step. Meanwhile, these independent parameters, in addition to stability, control the rate of accuracy and convergence compared to the exact solution.

Here we multiply two independent parameters γ and β in the last term of Eqs. (6) and (7), i.e., $\Delta\ddot{u}_{i+1}$. As u_t and $\dot{u}_t$ are the functions of $\ddot{u}_{t+\Delta t}$, independent parameters β and γ for controlling stability and accuracy are multiplied in acceleration term and, as a result, these adjustable parameters control stability and accuracy of the proposed method. Indeed, it causes some damping in the algorithm. So we rewrite Eqs. (6) and (7) as,

$$u_{i+1} = u_i + \Delta t\dot{u}_i + \frac{\Delta t^2}{2}\ddot{u}_i + \frac{\beta\Delta t^2}{6}\Delta\ddot{u}_{i+1} \tag{8}$$

and

$$\dot{u}_{i+1} = \dot{u}_i + \Delta t\ddot{u}_i + \frac{\gamma\Delta t}{2}\Delta\ddot{u}_{i+1} \tag{9}$$

In the above equations, $\Delta\ddot{u}_{i+1} = \ddot{u}_{i+1} - \ddot{u}_i$.

In order to write a computer code, Eqs. (8) and (9) can be written in an implicit form as below. In these equations, term $\Delta\ddot{u}_{i+1}$ is omitted.

$$u_{i+1} = u_i + \Delta t\dot{u}_i + \Delta t^2\left(\frac{1}{2} - \frac{\beta}{6}\right)\ddot{u}_i + \frac{\beta\Delta t^2}{6}\ddot{u}_{i+1} \tag{10a}$$

$$\dot{u}_{i+1} = \dot{u}_i + \Delta t\left(1 - \frac{\gamma}{2}\right)\ddot{u}_i + \frac{\gamma\Delta t}{2}\ddot{u}_{i+1} \tag{10b}$$

5 Analysis of Proposed Method

Stability, numerical dissipation and dispersion characteristics of an integration algorithm are generally analyzed by two approaches, namely, (1) recurrence relations using an amplification matrix or (2) discrete control theory (Belytschko and Hughes 1983). In this study, the first method will be used.

By investigating the properties of a numerical method such as convergence, stability, accuracy, the most favorable values of independent parameters such as γ and β can be obtained so that high accuracy is achieved while unconditionally stability is maintained. To establish the convergence of an algorithm in addition to stability, consistency and accuracy must be also considered. Measure of accuracy can be evaluated by investigating the numerical dissipation and dispersion (Belytschko and Hughes 1983; Volgers 1997).

5.1 Stability Analysis

Stability analysis of an integration algorithm applied to linear elastic systems is generally carried out by the amplification matrix approach. An amplification matrix is formed for an integration algorithm, and the algorithm is considered to be unconditionally stable if the spectral radius of the amplification matrix does not exceed the value of 1.0 for any value of $\omega_n\Delta t$, where ω_n is the highest natural frequency of the structure and Δt is the time step size used in the integration algorithm (Bathe 1996). Otherwise, the integration algorithm is considered to be conditionally stable. To this end, the equations of the proposed algorithms for a SDOF system under free-vibration can be represented by the following matrix recursive relationship:

$$\{\hat{X}_{t+\Delta t}\} = [A]\{\hat{X}_t\} + \{L\}\hat{f}_{t+\upsilon} \tag{11}$$

where $\hat{X}_{t+\Delta t}$ and $\hat{X}_t$ are vectors storing the solution quantities (e.g., displacements, velocities) and $\hat{f}_{t+\upsilon}$ is the load at time $t + v$. The v may be *0*, Δt or any other value that is different for each integration method. The matrix $\boldsymbol{A}$ is called amplification matrix (Bathe 1996).

Now, having Eqs. (10a) and (10b) in hand, it is possible to make the amplification matrix. The amplification matrix of each method can be ascertained by considering the SDOF model in the discrete time domain in $t + \Delta t(i+1)$ time instant as follows

$$\ddot{u}_{i+1} + 2\xi\omega\,\dot{u}_{i+1} + \omega^2 u_{i+1} = f_{i+1} \tag{12}$$

where ξ and ω are the damping ratio and natural frequency of the system, respectively and $f_{i+1} = F_{i+1}/m$. So that m is the mass of the system and F_{i+1} is external force applied to the system.

Inserting Eqs. (10a) and (10b) in Eq. (12), we get to an equation with $\ddot{u}_{i+1}$ as the only unknown. After simplification, this equation can be written as it is shown below

$$\ddot{u}_{i+1} = \left(2\kappa\left(\frac{\gamma}{2} - 1\right) + \mu\left(\frac{\beta}{6} - \frac{1}{2}\right)\right)\ddot{u}_i + \left(\frac{-2\kappa}{\Delta t} - \frac{\mu}{\Delta t}\right)\dot{u}_i - \frac{\mu}{\Delta t^2} + \frac{\mu f_{i+1}}{\omega^2 \Delta t^2} \tag{13}$$

where $\mu = \left(\frac{1}{\omega^2\Delta t^2} + \frac{\xi\gamma}{\omega\Delta t} + \frac{\beta}{6}\right)^{-1}$ and $\kappa = \frac{\xi\mu}{\omega\Delta t}$.

Equation (13) represents the acceleration at time instant $i+1$ in terms of all responses at time i. If we replace this equation with terms $\ddot{u}_{i+1}$ in Eq. (10), two equations will be obtained. These two equations and Eq. (13) make a relationship of the form of Eq. (11) as,

$$\begin{pmatrix} \ddot{u}_{t+\Delta t} \\ \dot{u}_{t+\Delta t} \\ u_{t+\Delta t} \end{pmatrix} = [A]\begin{pmatrix} \ddot{u}_t \\ \dot{u}_t \\ u_t \end{pmatrix}\{L\}f_{t+\Delta t} \tag{14}$$

According to the fact that the stability of an integration method is determined by examining the behavior of the numerical solution for arbitrary initial conditions, we consider the integration of Eq. (14) when no load is satisfied, i.e., $f = 0$ (Bathe 1996).

It can be shown mathematically that the response produced by the recursive relation in Eq. (14) for any arbitrary initial conditions and Δt will be bounded if the magnitude of all the eigenvalues of the amplification matrix in **A** are less than or equal to unity. In other words, the spectral radius of the amplification matrix $\rho(A) = \max(\lambda^i)$ where λ^i are the eigenvalues, is strictly less than unity, ensure bounded response, where the eigenvalues λ^i can be determined by solving the following eigenvalue problem.

Since the changes of damping ratio do not have much impact on variation of spectral radius, here, assume $\xi = 0$ in amplification matrix. So amplification matrix $\boldsymbol{A}$ in Eq. (14) is obtained as

$$A = \begin{bmatrix} \mu\left(\frac{\beta}{6} - \frac{1}{2}\right) & -\frac{\mu}{\Delta t} & \frac{-\mu}{\Delta t^2} \\ \Delta t\left(\left(1 - \frac{\gamma}{2}\right) + \frac{\mu\gamma}{2}\left(\frac{\beta}{6} - \frac{1}{2}\right)\right) & 1 - \frac{\gamma\mu}{2} & \frac{-\gamma\mu}{2\Delta t} \\ \Delta t^2\left(\left(\frac{1}{2} - \frac{\beta}{6}\right) + \frac{\mu\beta}{6}\left(\frac{\beta}{6} - \frac{1}{2}\right)\right) & \Delta t\left(1 - \frac{\gamma\mu}{2}\right) & 1 - \frac{\beta\mu}{6} \end{bmatrix} \tag{15}$$

where $\mu = \left(\frac{1}{\omega^2\Delta t^2} + \frac{\beta}{6}\right)^{-1}$ and ω is a natural frequency of the system.

$$|A - \lambda I| = \lambda^3 - 2A_1\lambda^2 + A_2\lambda - A_3 = 0 \tag{16}$$

where $\boldsymbol{I}$ is the identity matrix of dimension 3×3, $A_1 =$ trace of **A**, $A_2 =$ sum of 2×2 principal minors of **A**, and $A_3 =$ determinant of A. In the characteristic equation $A_3 = 0$, thus the vanished eigenvalue is $\lambda_3 = 0$ and the characteristic equation can be written as the following form:

$$\lambda^2 + a_1\lambda + a_2 = 0 \tag{17}$$

where

$$a_1 = \frac{\mu}{2}(1+\gamma) - 2 \tag{18}$$

and

$$a_2 = \frac{\mu}{2}(1-\gamma) + 1 \tag{19}$$

Stability of the proposed algorithm depends on the behavior of Eq. (17) (Belytschko and Hughes 1983). According to *Rough–Horwitz* criteria, in order for a dynamic system to be stable, all the roots of the characteristic equation of the eigenvalue problem must have negative real parts (Dorf and Bishop 1995). For Eq. (17), that roots of this equation are $\lambda_{1,2} = (-a_1 \pm \sqrt{a_1^2 - 4a_2})/2$. *Rough–Horwitz* criteria are confirmed when a_1 and a_2 are positive. So if the roots of the characteristic equation are real, both of them should be negative and if these roots are complex, both of them should have negative real parts. Considering $a_1 > 0$ complex conjugate roots of characteristic equation leads to $a_1^2 - 4a_2 \le 0$. According to the polar space, inserting a_1 and a_2 in $a_1^2 - 4a_2 \le 0$ helps to conclude that the characteristic equation has a pair of complex conjugate roots if

$$\mu \le \frac{16}{(\gamma+1)^2} \tag{20}$$

Due to the definition of μ, the above inequality is determinate when

$$\frac{1}{16}(\gamma+1)^2 - \frac{\beta}{6} \le \frac{1}{\omega_i^2\Delta t^2} \quad i = 1\ldots N \tag{21}$$

so, N is the number of system degrees of freedom. Due to the above conditions, solving the characteristic Eq. (17), the eigenvalues will be obtained as,

$$\lambda_{1,2} = \tilde{A} \pm i\tilde{B} \tag{22}$$

where

$$\tilde{A} = \frac{\mu}{4}(\gamma+1) - 1 \tag{23}$$

and

$$\tilde{B} = \frac{1}{4}\sqrt{\mu(\mu\gamma^2 + 2\mu\gamma + \mu - 16)} \quad (24)$$

The eigenvalues λ_1 and λ_2 in polar space can be written as,

$$\lambda_1, \lambda_2 = re^{i\theta}, \ \theta \in [0, 2\pi] \quad (25)$$

where $r = \sqrt{\tilde{A}^2 + \tilde{B}^2}$ and $\theta = \arctan(\tilde{B}/\tilde{A})$.

In order to have a stable numerical solution the spectral radius r must be less than 1.0, i.e., $r \leq 1$. So the stability condition is achieved as

$$r = \sqrt{1 + \frac{\mu}{2}(1-\gamma)} \leq 1 \quad (26)$$

Thus it is concluded that $\gamma \geq 1$. So the algorithm is stable if these conditions are satisfied. Meanwhile, according to Eq. (21), when $\omega\Delta t \to \infty$, unconditional stability can be obtained when,

$$\beta \geq \frac{3}{8}(\gamma+1)^2 \quad (27)$$

According to the conditions obtained from the above equations, Fig. 1 depicts stability bounds and regions for the proposed method. Figure 2 shows the variation of spectral radius in terms of variation of time step $\Delta t/T$ for different values of γ and β. As indicated in the graph, the proposed method is stable when the parameter γ is more than unity. However, parameter β is dependent on γ.

Figure 3 compares spectral radius of modified cubic B-spline method with previous version, conditionally stable cubic B-spline methods (Shojaee et al. 2011; Rostami et al. 2013). As it is clear, stability limit of cubic B-spline method is 0.55, while after stabilization, the spectral radius is less than unity for all values of $\Delta t/T$.

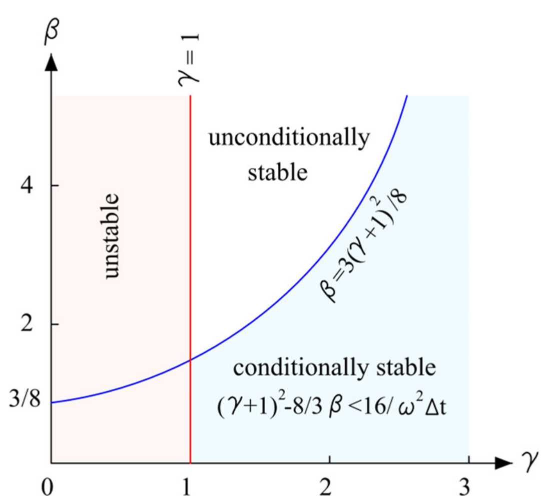

Fig. 1 Stability bounds and regions

5.2 Consistency and Convergence

A time integration scheme is said to be consistent if (Rio et al. 2005):

$$\lim_{\Delta t \to 0.0} \frac{u_{t+\Delta t} - u_t}{\Delta t} = \dot{u}_t, \ \lim_{\Delta t \to 0.0} \frac{\dot{u}_{t+\Delta t} - \dot{u}_t}{\Delta t} = \ddot{u}_t \quad (28)$$

Checking the above relation for the proposed method will result in

$$\lim_{\Delta t \to 0} \begin{bmatrix} \frac{\dot{u}_{t+\Delta t} - \dot{u}_t}{\Delta t} \\ \frac{u_{t+\Delta t} - u_t}{\Delta t} \end{bmatrix} = \lim_{\Delta t \to 0} \begin{bmatrix} \left(1 - \frac{\gamma}{2}\right)\ddot{u}_t + \frac{1}{2}\ddot{u}_t\gamma \\ \dot{u}_t + \Delta t\left(\frac{1}{2} - \frac{\beta}{6}\right)\ddot{u}_t + \frac{\Delta t}{6}\ddot{u}_t\beta \end{bmatrix} = \begin{bmatrix} \ddot{u}_t \\ \dot{u}_t \end{bmatrix} \quad (29)$$

It is shown that the proposed method is consistent for all values of γ and β parameters but order of accuracy should be determined for this new scheme.

The algorithm is convergent if for a fixed $t_n = n\Delta t$ the displacement value u_n equals the true solution of Eq. (12) (when no load is satisfied, i.e.,$f = 0$) in the limit $n = \infty$, $\Delta t = 0$.

Many important properties of an integration algorithm can be determined from the spectral properties of its amplification matrix $\boldsymbol{A}$. Equation (16) represents the characteristic equation for $\boldsymbol{A}$, as the invariants of $\boldsymbol{A}$ are:

$$A_1 = 1 - \frac{\mu}{4}(1+\gamma) \quad (30)$$

$$A_2 = 1 + \frac{\mu}{2}(1-\gamma) \quad (31)$$

Expanding Eq. (14), in form $\{\hat{X}_{t+\Delta t}\} = [A]\{\hat{X}_t\}$, for three consecutive time steps of equal length Δt, velocities and accelerations may be eliminated leading to difference equation in terms of the displacements:

$$u_{n+1} - 2A_1u_n + A_2u_{n-1} - A_3u_{n-2} = 0 \ n \in \{2, 3, \ldots, N-1\} \quad (32)$$

Comparison of Eq. (32) with (16) demonstrates that the discrete solution has the representation

$$u_n = \sum_{i=1}^{3} c_i\lambda_i^n \quad (33)$$

where c_1 to c_3 depend on the initial conditions.

The *local truncation error* of (32) is

$$\sigma = [u(t+\Delta t) - 2A_1u(t) + A_2u(t-\Delta t) - A_3u(t-2\Delta t)]/\Delta t^2 \quad (34)$$

where u satisfies the equilibrium equation.

Using derivation of u and Taylor expanding u about t, Eq. (34) can be written as:

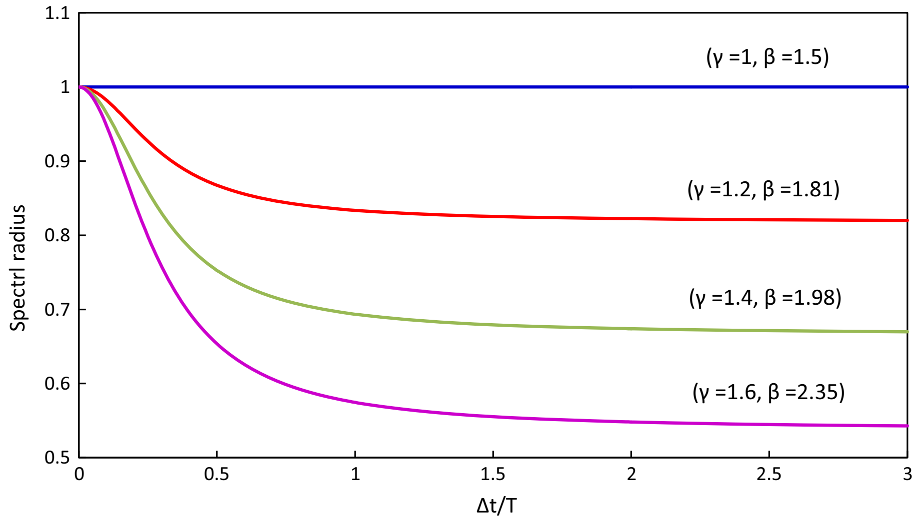

Fig. 2 Variation of spectral radius in terms of variation of $\Delta t/T$

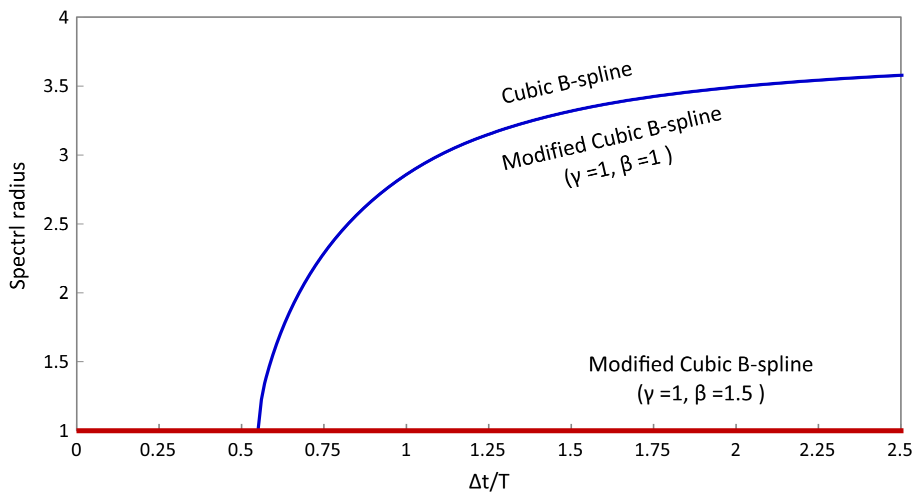

Fig. 3 Comparison of spectral radius for proposed method with previous versions

$$\sigma = \sum_{i=0}^{m} T_i \Delta t^{i-2} u^{(i)}(t) + O(\Delta t^{m-1}) \tag{35}$$

where

$$T_0 = 1 - 2A_1 + A_2 - A_3 \tag{36}$$

$$T_i = \left[1 - (-1)^i A_2 - (-2)^i A_3\right]/i! \tag{37}$$

The difference Eq. (32) is said to be consistent with the differential Eq. (12) if $\sigma = O(\Delta t)^k$ in which k is called the order of accuracy.

Since u satisfies homogeneous SDOF model equation $m\ddot{u} + ku = 0$ (i.e., Eq. (12) with $f = 0$ and $\xi = 0$), all derivatives in (35) of second and higher order can be eliminated. Setting $m = 4$ in (35) and eliminating higher-order derivations yields

$$\sigma = \left(\Omega^{-2}T_0 - T_2 + \Omega^2 T_4\right)\omega^2 u + \left(\Omega^{-1}T_1 - \Omega T_3\right)\omega^2 \dot{u} + O(\Delta t^3) \tag{38}$$

In which $\Omega = \omega\Delta t$, $T_0 = \mu$ and $T_1 - T_4$ are defined by

$$T_1 = -\frac{\mu}{2}(1-\gamma) \tag{39a}$$

$$T_2 = 1 + \frac{\mu}{4}(1-\gamma) \tag{39b}$$

$$T_3 = \frac{T_1}{3!} \tag{39c}$$

$$T_4 = \frac{1}{4!}(2T_2) \tag{39d}$$

Employing the above in Eq. (38) reveals that

$$\sigma = \left[-\frac{\mu}{2}(1-\gamma)\left(\frac{1}{\Delta t} - \frac{\omega^2\Delta t}{3!}\right)\right]\dot{u} + O\Delta t^2 \tag{40}$$

It is clear from Eq. (40) with no restrictions on γ and β the difference equation is consistent and first-order accurate. However, if $\gamma = 1$ the order of accuracy is at least 2, i.e., $O\Delta t^2$. Assuming this is the case, Eq. (38) becomes

$$\sigma = \left(\frac{\mu}{\Delta t^2} - \omega^2 + \frac{\Omega^2}{4!}\right)u + O\Delta t^3 \tag{41}$$

Thus the order of accuracy is at least 3, i.e., $O\Delta t^3$, if

$$\beta = \frac{6}{\Omega}\left(\frac{1}{(1-\Delta t^2/24)} - 1\right) \tag{42}$$

So the above equation indicates that, to have second-order order accuracy, β should be selected based on model frequency and specified time step.

5.3 Dissipation and Dispersion

Evaluation of dissipation and dispersion error is another factor for determination of the efficiency of a method. That is, we should evaluate the amplitude decay and period elongation for a periodical dynamics. The solution of Eq. (16) or (32) may has two conjugate complex roots. Denote the complex roots by λ_1 and λ_2 are principal. They can be expressed as follows [see also (Hilber 1976)]:

$$\lambda_{1,2} = \tilde{A} \pm i\tilde{B} = \exp\left(-\bar{\Omega}\left(\bar{\xi} \pm i\sqrt{1-\xi^2}\right)\right) \tag{43}$$

where $\tilde{A}$ and $\tilde{B}$ are real [defined in Eq. (22)] and $i = \sqrt{-1}$. The coefficients $\bar{\Omega}$ and $\bar{\xi}$ are defined by

$$\bar{\Omega} = \operatorname{arctg}(\tilde{B}/\tilde{A})/\sqrt{1-\xi^2} \tag{44}$$

$$\bar{\xi} = -\ln(\tilde{A}^2 + \tilde{B}^2)/2\bar{\Omega} \tag{45}$$

Substituting Eq. (43) in (33), the following expression for u is obtained

$$u_n = \exp\left(-\bar{\xi}\bar{\omega}t_n\right)\left[c_1' \cos\bar{\omega}_d t_n + c_2' \sin\bar{\omega}_d t_n\right] + c_3\lambda_3^n \tag{46}$$

where $\bar{\omega} = \bar{\Omega}/\Delta t$ and $\bar{\omega}_d = \bar{\omega}\sqrt{1-\xi^2}$. The constant c_1' and c_2' are determined from the initial conditions. As the influence of the spurious root λ_3 vanishes in the limit $\Delta t = 0$ for convergent algorithms, Eq. (46) shows that the quantity $\bar{\xi}$ can be used as a measure of the numerically dissipated energy. $\bar{\xi}$ will be called the *algorithmic damping* ratio (dissipation) in analogy to the physical damping ratio ξ. Some references used *amplitude decay* (AD) instead of $\bar{\xi}$ so that $\bar{\xi} = \mathrm{AD}/2\pi$. The parameter τ also defined by

$$\tau = \frac{\bar{T} - T}{T} = \left(\frac{\omega}{\bar{\omega}} - 1\right) \tag{47}$$

$T = 2\pi/\omega$, and $\bar{T} = 2\pi/\bar{\omega}$ are convenient measures of frequency distortion (dispersion) numerically introduced by the algorithm. τ will be called the *relative period error* (TD).

According to Eq. (45), $\tilde{A}^2 + \tilde{B}^2 = 1$ leads to no dissipation for method, i.e., $\mathrm{AD} = 0$. The result will be $\gamma = 1$ for the proposed method. The error related to the numerical damping or, in other words, the rate of amplitude decay, has been investigated for the proposed method. Figure 4 shows algorithmic damping ratio in terms of $\Delta t/T$ for different values of γ higher than one. As it is clear from the graphs, for $\gamma = 1$ the proposed method behaves without numerical damping.

In order to achieve maximum accuracy, relative period error (TD) has been determined while no algorithmic damping exists ($\gamma = 1$). In this case, TD depends on both the independent parameter β and time step Δt. Figure 5 plots the curves of the relative error of period versus the ratio of $\Delta t/T$ for different parameter β in the region of 0.1–1.5.

The data in Figs. 4 and 5 show that for the integration methods, the magnitude of error measurements usually increases when the time step Δt increases. The most favorable value of β is 1.5 and it is obtained when algorithmic damping is nonexistent (i.e., $\gamma = 1$) because it leads to the minimum value of relative period error. Although choosing β less than 1.5 leads to decrease in dispersion error, it should be noted that lower values do not guarantee the unconditional stability. It should be noted that, the results in the proposed method with $\gamma = 1$ and $\beta = 1.5$ are perfectly adapted to results of Newmark method with $\gamma = 1/2$ and $\beta = 1/4$. Figures 6 and 7 show this issue clearly. In these figures, 'MCB-Spline' is the abbreviation standing for proposed modified cubic B-spline method.

5.4 Solution Algorithm

In order to write a computer code, the complete algorithm used in this proposed method is summarized in Table 2. This algorithm was obtained after doing a series of algebraic calculations on Eq. (10) which are not presented here.

If we compare this algorithm with the same algorithm presented for cubic B-spline method in Rostami et al. (2013), it will be recognized that the new procedure is summarized and much simpler.

6 Numerical Evaluation

In this section, the validity of the proposed method is confirmed with examination of several results. Two examples are considered, including a three degrees-of-freedom spring system and a triple layer space truss structure. The first example is a special 'model problem,'

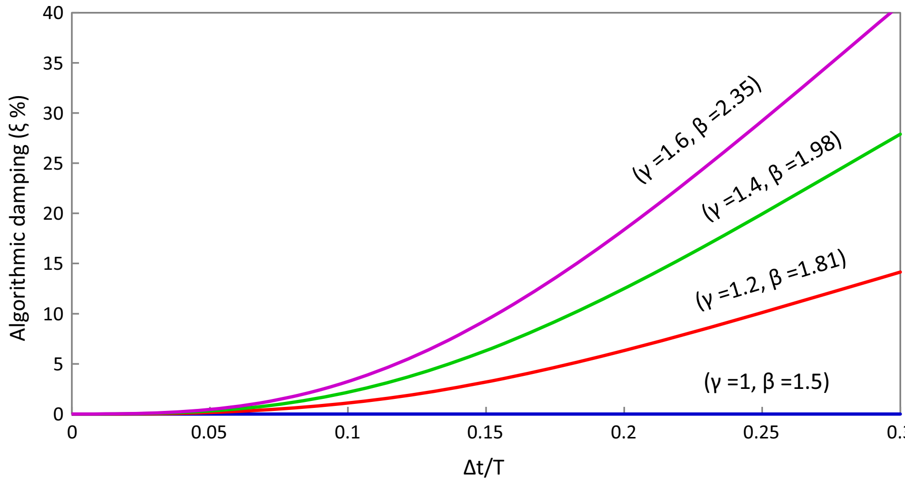

Fig. 4 Curves of algorithmic damping versus the dimensionless time step $\Delta t/T$ for various values of γ

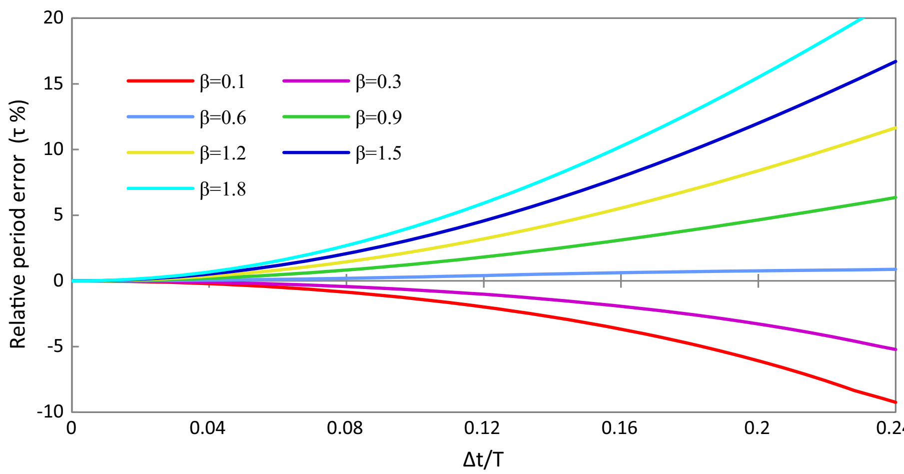

Fig. 5 Curves of relative period error versus the dimensionless time step $\Delta t/T$ for various values of β

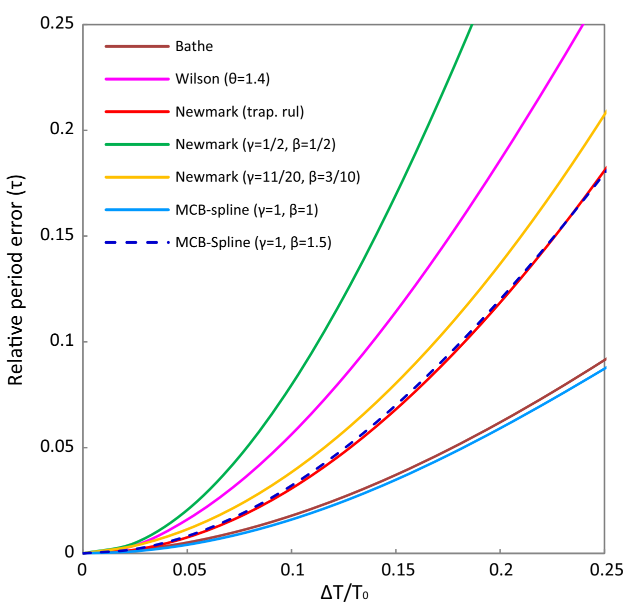

Fig. 6 Relative period error (period dispersion)

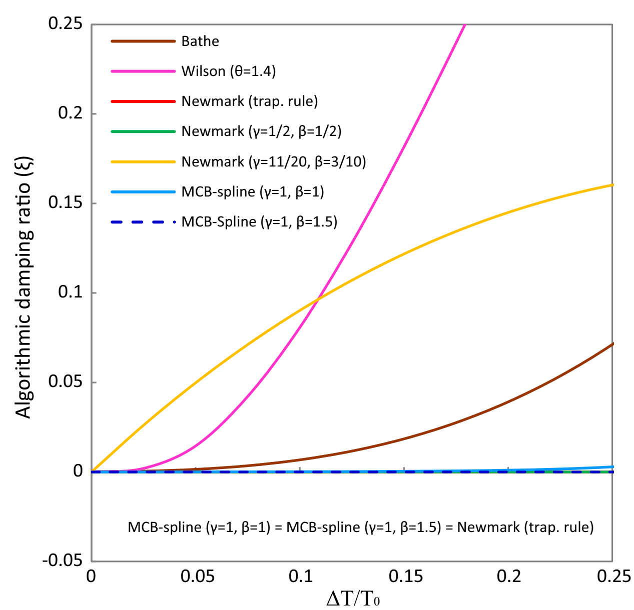

Fig. 7 Algorithmic damping (dissipation)

Table 2 Proposed step-by-step implicit algorithm (modified cubic B-spline method)

A. Initial calculation

Form stiffness matrix K, mass matrix M and damping matrix C of the system

Specify the vector of applied forces to the system F, in each time instant

Initialize U_0 and $\dot{U}_0$

Select time step Δt and parameters γ and β, then calculate integration constants

$\gamma \geq 1;\ \beta \geq \frac{3}{8}(\gamma + 1)^2$

$$a_0 = \frac{6}{\beta \Delta t^2}; \quad a_1 = \frac{3\gamma}{\beta \Delta t}; \quad a_2 = \Delta t a_0; \quad a_3 = \frac{3}{\beta} - 1;$$

$$a_4 = a_1 \Delta t - 1; \quad a_5 = \Delta t\left(\frac{3\gamma}{2\beta} - 1\right); \quad a_6 = \Delta t\left(1 - \frac{2}{\gamma}\right); \quad a_7 = \frac{\Delta t}{2}\gamma;$$

Form effective stiffness matrix $\hat{K}$

$\hat{K} = K + a_0 M + a_1 C$

Triangularize $\hat{K}$: $\hat{K} = LDL^{\mathrm{T}}$

B. For each time step $(i = 0,1,\ldots,n)$

Calculate effective loads at time $t + \Delta t$

$\hat{F}_{t+\Delta t} = F_{t+\Delta t} + M(a_0 u_t + a_2 \dot{u}_t + a_3 \ddot{u}_t) + C(a_1 u_t + a_4 \dot{u}_t + a_5 \ddot{u}_t)$

Solve for displacements at time $t + \Delta t$:

$\hat{K}\, u_{t+\Delta t} = \hat{F}_{t+\Delta t}$

Calculate velocities, accelerations at time $t + \Delta t$

$\ddot{u}_{t+\Delta t} = a_0(u_{t+\Delta t} - u_t) - a_2 \dot{u}_t - a_3 \ddot{u}_t$

$\dot{u}_{t+\Delta t} = \dot{u}_t + a_6 \ddot{u}_t + a_7 \ddot{u}_{t+\Delta t}$

which is very convenient to test the accuracy of numerical methods and studying the behavior of the numerical solution when obtaining via the direct integration method is desired. The second example is a large scale problem to test computational cost of the integration methods.

6.1 Three Degrees-of-Freedom Spring System

The objective of this section is to present the solution for a simple linear system that has been evaluated by use of Bathe and Noh (2013). The calculated solution shows the value of the method. The solution of the three degrees-of-freedom spring system is considered and shown in Fig. 8 for which node 1 is subject to the prescribed displacement over time. The governing equation can be rewritten to solve only the unknown displacements u_2 and u_3. For this system, $k_1 = 10^7$, $k_2 = 1$, $m_1 = 0$, $m_2 = 1$, $m_3 = 1$ are considered and the displacement is prescribed at node 1 to be $u_1 = \sin \omega_{\mathrm{p}} t$ with $\omega_{\mathrm{p}} = 1.2$.

The important point to note is that this simple problem as a 'model problem' represent the stiff and flexible parts of a much more complex structural system. In a mode superposition solution, the response within these stiff parts (a response that corresponds to very high artificial frequencies) would naturally not be included. In fact, the system shown in Fig. 8 is used as a 'model system' of such complex structural systems of many thousands of degrees of freedom and studying the behavior of the numerical solution when obtained by the direct integration method is desired. In this example, the spring system is considered using zero initial conditions for the displacements and velocities at nodes 2 and 3 (as must typically be done in a complex many degrees-of-freedom structural analysis) and is solved for the response over 10 s. Time-stepping algorithm for the solution of this system is used. The time step used is $\Delta t = 0.2618$; hence, $\Delta t / T_1 = 0.0417$ and $\Delta t / T_2 = 131.76$, where $T_1 = 6.283$, $T_2 = 0.002$ are the natural periods of the system with two degrees of freedom.

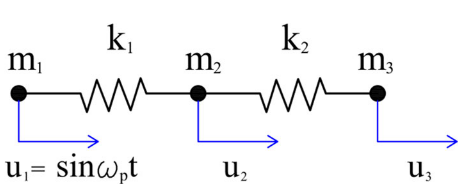

Fig. 8 Model problem of three degrees-of-freedom spring system

Figures 9, 10, 11, 12, 13 and 14 show the calculated solutions of node 2. Because for solutions of node 3 the responses of all numerical methods are to close, here only the node 2 is investigated. These figures also give the response obtained in a mode superposition solution, referred to as 'reference solution' using only the lowest frequency mode plus the static correction (Bathe and Noh 2012).

Figures show that in all time-stepping schemes, the proposed and the Bathe methods perform very well; particularly, the velocity and acceleration at node 2 are very well predicted. But it should be noted that the Bathe method is a two-step method where for each time step, trapezoidal rule is used

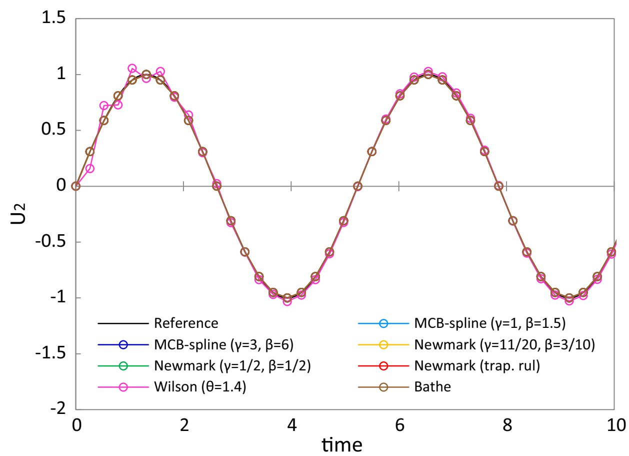

Fig. 9 Displacement of node 2 for different methods

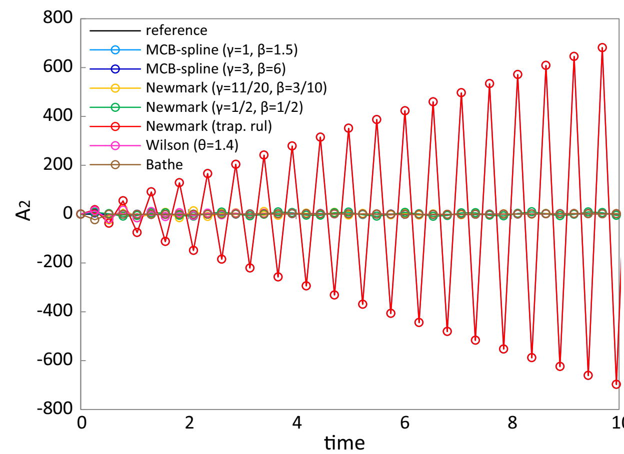

Fig. 12 Acceleration of node 2 for different methods

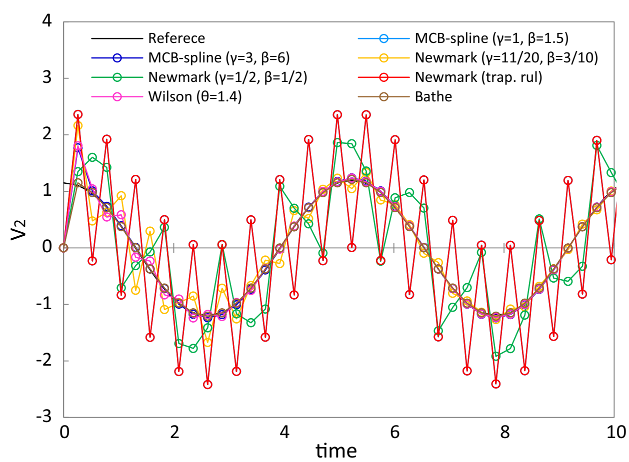

Fig. 10 Velocity of node 2 for different methods

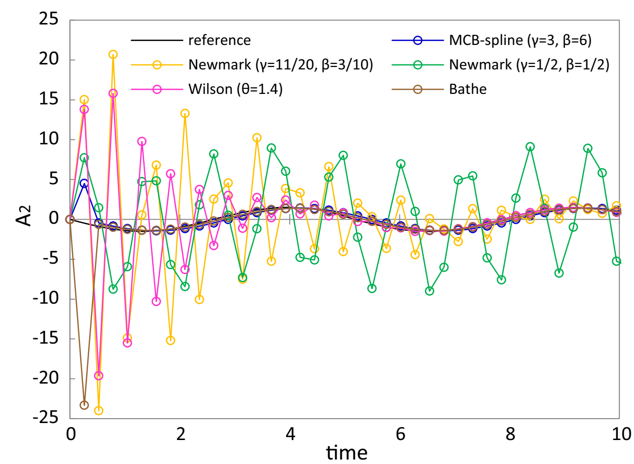

Fig. 13 Acceleration of node 2 for different methods

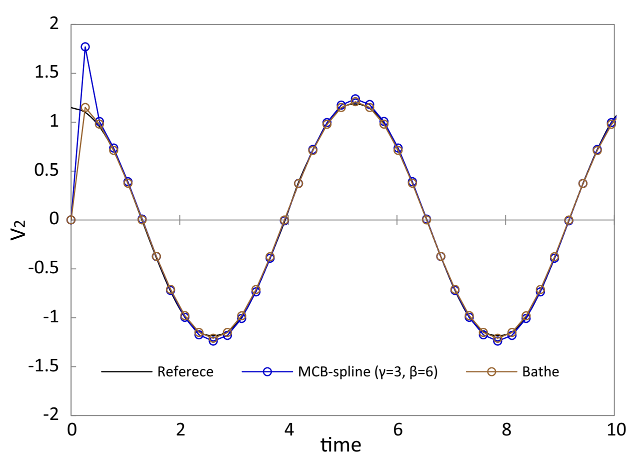

Fig. 11 Velocity of node 2 for different methods

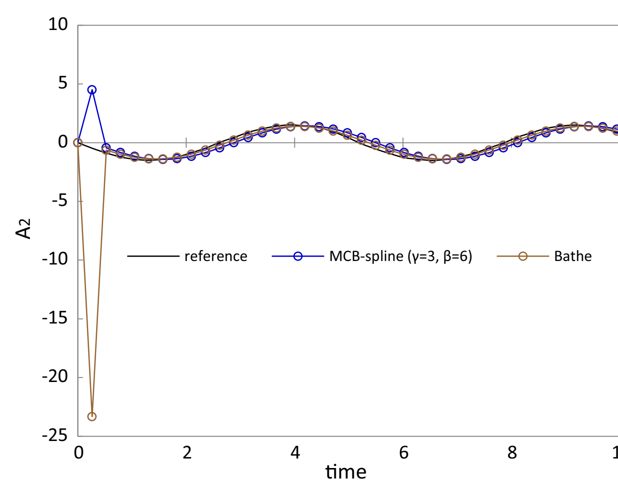

Fig. 14 Acceleration of node 2 for different methods

in the first half-step and three point backward difference method is used in the second half-step (Bathe 2007; Bathe and Noh 2012). However, all other methods under study in this paper are one-step. In fact, the trapezoidal rule displays large errors and instability in the calculation of the acceleration at node 2, see Fig. 12. Some methods were omitted in

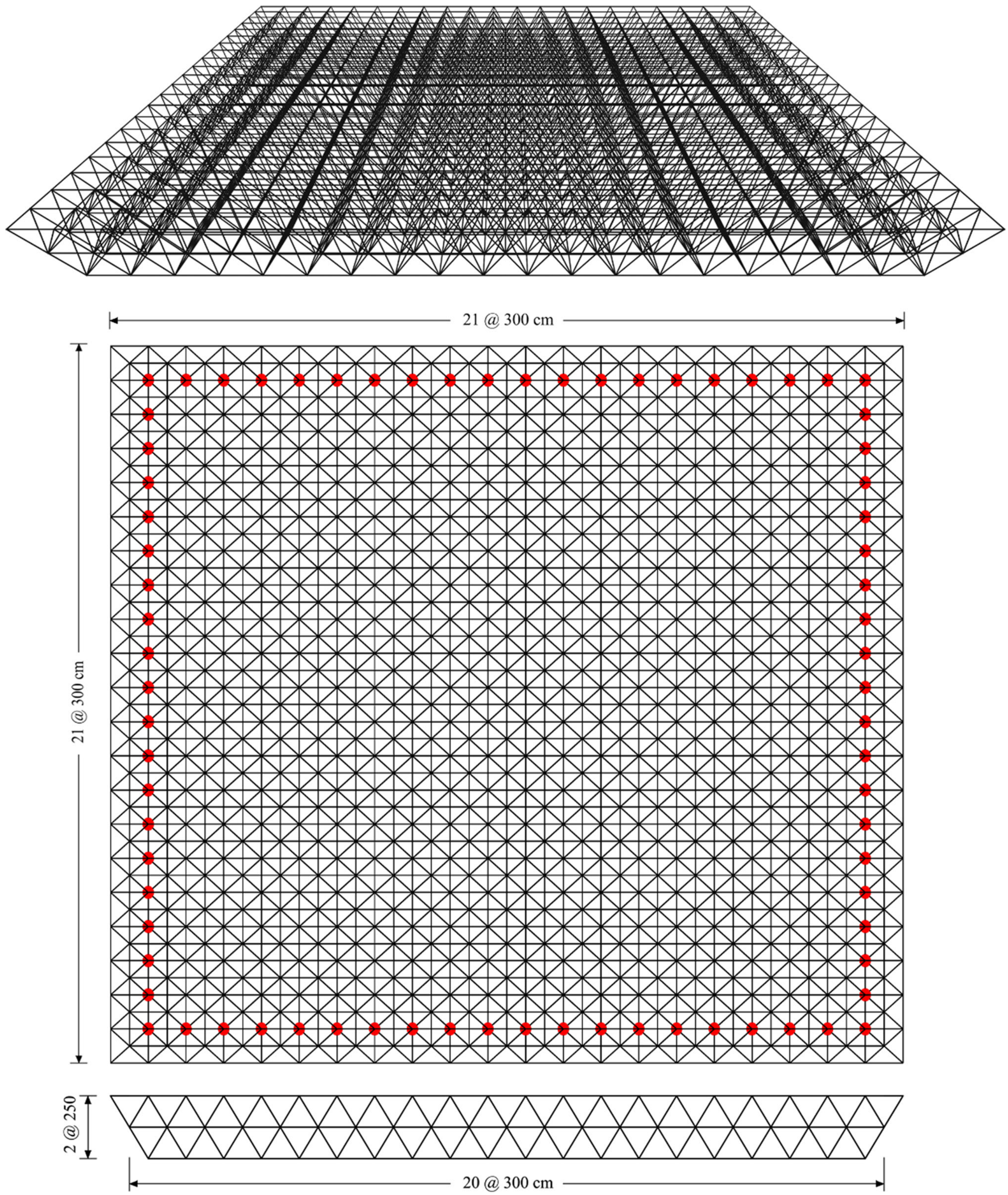

Fig. 15 Configuration of triple layer spatial structure (section, plan and 3-D view)

Figs. 11, 13 and 14 in order to make the comparison easier. In Fig. 14, the first step error in the proposed method is less than that in the Bathe method. Solving this example with the proposed method, unlike the basic method which was the subject of researches developed by Shojaee et al. (2011) and Rostami et al. (2013), shows that the modified cubic B-spline method always maintains its stability and shows high accuracy.

6.2 Triple Layer Grid (TLG) Structure Under Earthquake Load

The configuration and dimensions of a structure shown in Fig. 15 are plan and 3D view of a space truss that has been retrieved from Mashayekhi et al. (2016). The model is a triple layer spatial structure with 76 supports in the edges of the bottom layer. The structure is composed of 5888 members connected by 1325 nodes (joints). The total depth of the structure is 5 m, while the node spacing of top, middle and bottom chords is 3 m. The total length of the lower, middle and upper layers is 57, 60 and 63 m in both directions, respectively. All members in the structure are steel pipes with 16.4 cm as outside diameter and 0.45 cm thickness. The elastic modulus is 2.06×10^{10} kg/m^2 and mass density is 7850 kg/m^3. The El-Centro earthquake record as shown in Fig. 16 is used as vertical ground motion input data.$\Delta t = 0.02$ s has been selected as the time increment. In the analysis, the damping matrix is derived based on the mass matrix and the damping ratio of all 3474 modes of the structure so that the equivalent viscous damping ratio is equal to 5% for all modes (Paz and Leigh 2003). The maximum and minimum period of this system is 0.702 and 0.0088 s, respectively.

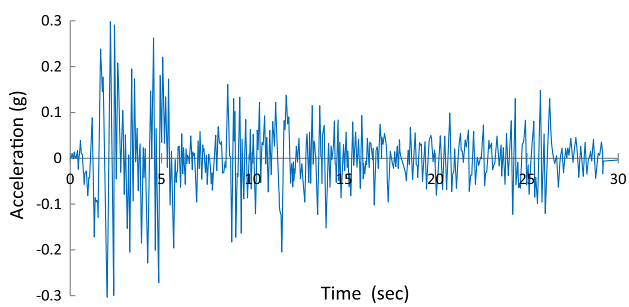

Fig. 16 El-Centro earthquake record

This example has been also analyzed by the methods which were used in the previous example. The 'Reference' is the mode superposition method with considering all modes in which the separated equations are being solved through the numerical solution of Duhamel integration method (Paz and Leigh 2003). An accuracy analysis with computational time consumption has been performed by use of a computer (Core i7 CPU @ 2.2 GHz). These analyses have been performed for 30 s after the earthquake is applied. The results including the values of vertical displacements, velocity and acceleration of the joint in the center of the middle layer have been depicted in Figs. 17, 18 and 19. All results are in terms of meter and second.

Because the time step Δt is small, the results of all numerical methods are close together. Although the purpose of choosing this issue unlike the previous example is evaluation of time consumption rate for all methods, for the sake of accuracy, we investigate the percentage error in the computed extreme response values. Table 3 shows peak value computational percentage error and time consumption analysis. It is clear from the table that Bathe method, trapezoidal rule and the proposed method bring a high accuracy; meanwhile, the Bathe method takes twice as much time as the proposed method to solve this problem. The results obtained from this analysis are demonstrated in Table 3. This example shows the efficiency and speed of the proposed method.

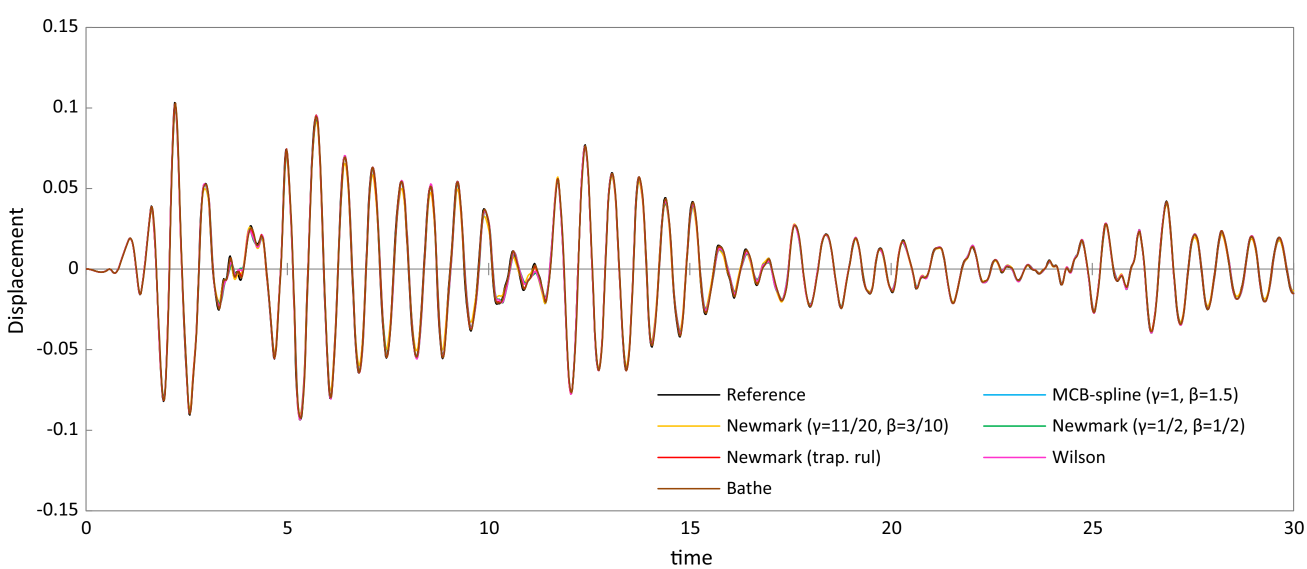

Fig. 17 Vertical displacement time history at middle joint for given methods

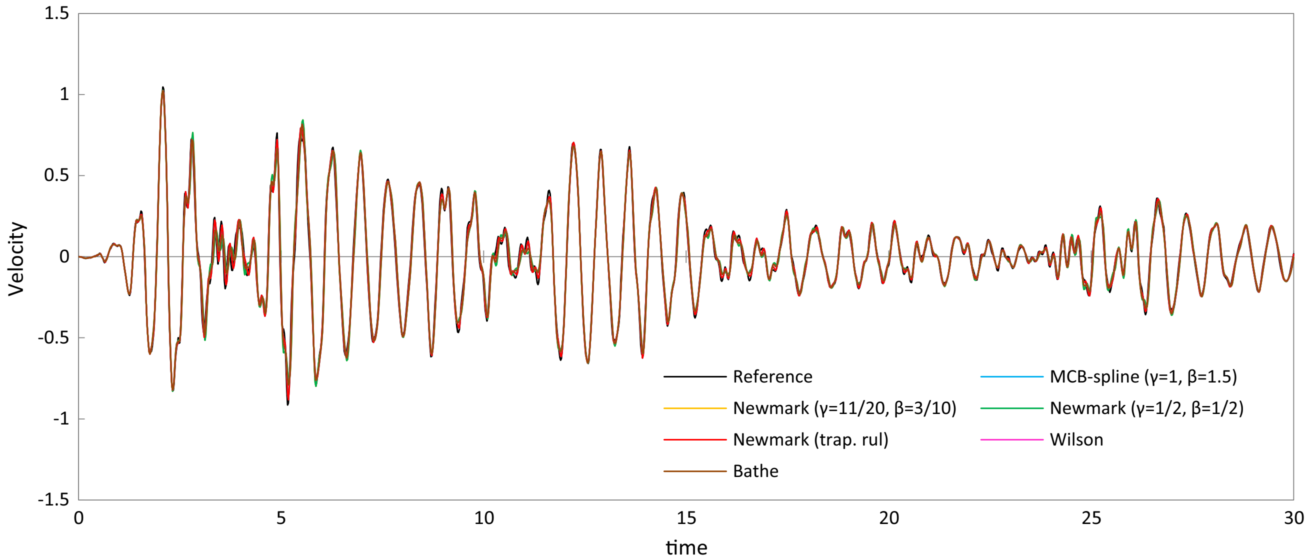

Fig. 18 Vertical velocity time history at middle joint for given methods

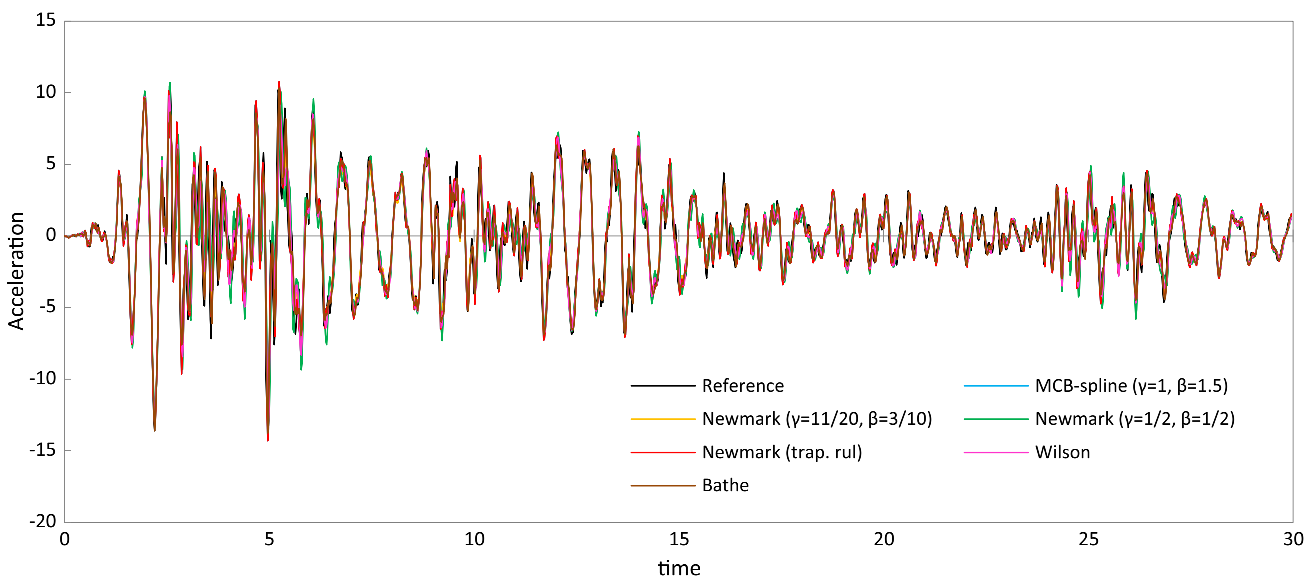

Fig. 19 Vertical acceleration time history at middle joint for given methods

7 Summary and Conclusions

The purpose of this paper was to present a scheme where the recent proposed conditionally stable cubic B-spline explicit time integration method is developed to an unconditionally stable state. A series of new formulas are extracted and by inserting two controlling parameters γ and β in the formulas, unconditional stability is guaranteed. The values of these two parameters have been determined to not only maintain the stability but also ensure the desired accuracy. It is found that the new scheme can achieve lower numerical amplitude dissipation and period dispersion compared to Wilson's method and trapezoidal rule. The new implicit scheme is simple and effective, and certainly practical when the trapezoidal rule is not effective or even fails. Numerical evaluations showed that the proposed method maintains its stability even in analysis of structures with high frequencies so that in the field of accuracy, the proposed method operates as well as the Bathe method. In addition, time consumption is reasonable in the proposed method; for a large scale problem, the proposed

Table 3 Percentage error estimation and time consumption (s) analysis for example 6.2

	Bathe	Wilson ($\theta = 1.4$)	Newmark (trap. rul)	Newmark $\left(\gamma = \frac{1}{2}, \beta = \frac{1}{2}\right)$	Newmark $\left(\gamma = \frac{11}{20}, \beta = \frac{3}{10}\right)$	MCB-spline ($\gamma = 1, \beta = 1.5$)
Dis. err. %						
Max	0.32	1.39	0.79	3.21	2.92	0.79
Min	0.61	0.56	0.78	0.63	3.02	0.78
Vel. err. %						
Max	1.54	2.21	2.26	1.94	3.07	2.26
Min	3.02	10.11	3.57	9.29	10.64	3.57
Acc. err. %						
Max	3.45	8.37	0.67	0.13	10.84	0.67
Min	1.23	2.58	5.14	2.45	1.14	5.14
Time (s)						
	46	23	21	21	21	20

method solved the problem in less than half the time taken by the Bathe method. Due to its unconditional stability, the proposed implicit technique is an excellent option for the time integration of a wide range of dynamic problems.

References

Bathe KJ (1996) Finite element procedures. Prentice Hall, Englewood Cliffs

Bathe KJ (2007) Conserving energy and momentum in nonlinear dynamics: a simple implicit time integration scheme. Comput Struct 85:437–445

Bathe KJ, Noh G (2012) Insight into an implicit time integration scheme for structural dynamics. Comput Struct 98:1–6

Belytschko T, Hughes TJR (eds) (1983) Computational methods for transient analysis: computational method in mechanics series, vol 1. North-Holland, Amsterdam

Chopra A (2007) Dynamics of structures: theory and applications to earthquake engineering, 3rd edn. Prentice Hall, Upper Saddle River

Dokainish MA, Subbaraj K (1989) A survey of direct time integration methods in computational structural dynamics. I. EXPLICIT methods. Comput Struct 32(6):1371–1386

Dorf RC, Bishop RH (1995) Modern control systems, 7th edn. Addision-Wesley, Reading, MA

Hilber HM (1976) Analysis and design of numerical integration methods in structural dynamics. Report No. EERC 76-29, Earthquake Engineering Research Center, University of California, Berkeley, California

Hilber HM, Hughes TJR (1978) Collocation, dissipation and 'overshoot' for time integration schemes in structural dynamics. Earthq Eng Struct Dyn 6:99–117

Hilber HM, Hughes TJR, Taylor RL (1977) Improved numerical dissipation for time integration algorithms in structural mechanics. Earthq Eng Struct Dyn 5(3):283–292

Kolay C, Ricles JM (2014) Development of a family of unconditionally stable explicit direct integration algorithms with controllable numerical energy dissipation. Earthq Eng Struct Dyn 43(9):1361–1380

Leontyev VA (2010) Direct time integration algorithm with controllable numerical dissipation for structural dynamics: two-step Lambda method. Appl Numer Math 60:277–292

Mashayekhi M, Salajegheh E, Dehghan M (2016) Topology optimization of double and triple layer grid structures using a modified gravitational harmony search algorithm with efficient member grouping strategy. Comput Struct 172:40–58

Newmark NM (1959) A method of computational for structural dynamics. J Eng Mech Div ASCE 85(3):67–94

Noh G, Bathe KJ (2013) An explicit time integration scheme for the analysis of wave propagations. Comput Struct 129:178–193

Paz M, Leigh W (2003) Structural dynamics: theory and computation. Springer, New York

Rio G, Soive A, Grolleau V (2005) Comparative study of numerical explicit time integration algorithms. Adv Eng Softw 36:252–265

Rostami S, Shojaee S, Moeinadini A (2012) A parabolic acceleration time integration method for structural dynamics using quartic B-spline functions. Appl Math Model 36(11):5162–5182

Rostami S, Shojaee S, Saffari H (2013) An explicit time integration method for structural dynamics using cubic B-spline polynomial function. Sci Iran Trans A Civ Eng 20(1):23–33

Shojaee S, Rostami S, Moeinadini A (2011) The numerical solution of dynamic response of SDOF systems using cubic B-spline polynomial functions. Struct Eng Mech 38(2):211–229

Shojaee S, Rostami S, Abbasi A (2015) An unconditionally stable implicit time integration algorithm: modified quartic B-spline method. Comput Struct 153:98–111

Soleymani SS, Noorzad A, Ansari A (2009) A time integration algorithm for linear transient analysis based on the reproducing kernel method. Comput Method Appl Mech Eng 198:3361–3377

Subbaraj K, Dokainish MA (1989) A survey of direct time integration methods in computational structural dynamics. II. Implicit methods. Comput Struct 32(6):1387–1401

Volgers PTG (1997) Development in B2000: a review of time integration methods. Technical report, Delft University of technology

Wang MF, Au FTK (2004) Higher-order mixed method for time integration in dynamic structural analysis. J Sound Vib 278:690–698

Wen WB, Jian KL, Luo SM (2014) An explicit time integration method for structural dynamics using septuple B-spline functions. Numer Methods Eng 97:629–657

Wen WB, Luo SM, Jian KL (2015) A novel time integration method for structural dynamics utilizing uniform quintic B-spline functions. Arch Appl Mech 85:1743–1759

Wilson EL (1986) A computer program for the dynamic stress analysis of underground structures. SESM Report No. 68-1. Division of Structural Engineering and Structural Mechanics, University of California, Berkeley, California

Wilson EL, Farhoomand I, Bathe KJ (1973) Nonlinear dynamic analysis of complex structures. Earthq Eng Struct Dyn 1(3):241–252

Wood WL, Bossak M, Zienkiewicz OC (1981) An alpha modification of Newmark's method. Numer Methods Eng 15:1562–1566